Relativistic and non-relativistic shock acceleration in various objects

R. Schlickeiser
Institut für Theoretische Physik
Lehrstuhl IV: Weltraum- und Astrophysik
Ruhr-Universität Bochum, Germany

I) Introduction
II) Standard Model of particle acceleration
III) Theory of test-particle acceleration in relativistic and non-relativ. flows
IV) Test-particle acceleration at non-relativistic parallel shocks
V) Clues from non-relativistic shock acceleration work
VI) Relativistic pick-up model
VII) Impact of future TeV observations
VIII) Conclusions

I) Introduction

3 types of explosive astrophysical events are of interest to H.E.S.S. observations:

Supernova explosions

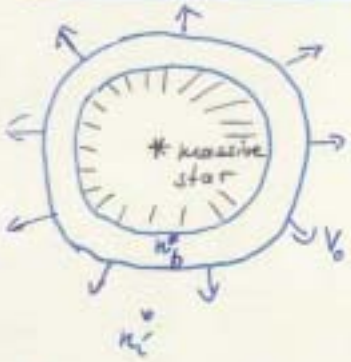

spherical outflow into interstellar medium,

nonrelativistic velocity $V_0 \ll c$

Gamma ray bursts = (hypernova, supernova)

anisotropic outflow into interstellar medium,

relativistic velocity $\Gamma_0 = \frac{1}{\sqrt{1-\frac{V_0^2}{c^2}}} \gg 1$

$\Gamma_0 \approx 300$

From combination of high luminosities ($\simeq 10^{50}$ erg s^{-1}) and short variability ($\gtrsim 10^{-3}$ s)

AGN jets

channeled (collimated) outflow into dynamic jet medium (= interstellar medium?)

$\Gamma_0 = 10$

How is kinetic energy of outflows converted to radiation?

GeV-TeV Cerenkov telescopes are sensitive to nonthermal emission from relativistic charged particles:

protons and hadrons	electrons and positrons
P1) π^0-decay P2) Proton synchrotron radiation P3) Suprathermal proton bremsstrahlung P4) secondary pair generation from $\pi^\pm$-decay (accompanied by neutrino production) followed by (E1)-(E3) of secondary pairs	E1) inverse Compton scattering of "low-energy" (mm – X-rays) target photons E2) nonthermal bremsstrahlung E3) pair annihilation

⇒ Yield in GeV-TeV photons determined by efficiency of acceleration processes of radiating charged particles!

Available free energy = Kinetic outflow energy in supernova explosions, gamma-ray bursts and AGN jets

Relevant dissipation processes of outflows in ambient cosmic plasmas:

- 2-stream instabilities of dense outflow plasma in dilute collisionless interstellar gas ($n_b^* \gg n_i^*$)
- formation of magnetized shock waves in collisionless environment (is hydrodynamic description of shock waves still valid at these scales?)

Dermer, Sturner, Schlickeiser 1997

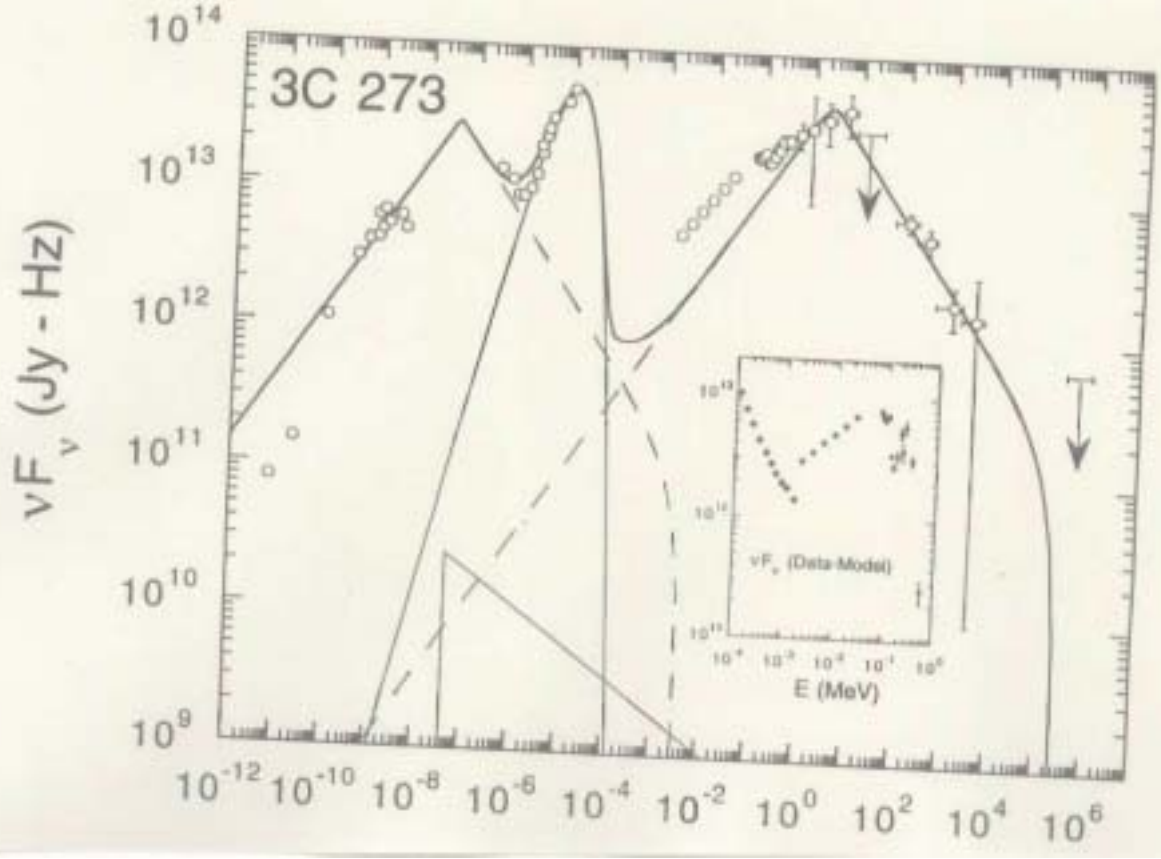

Fig. 12

M. Böttcher 1999

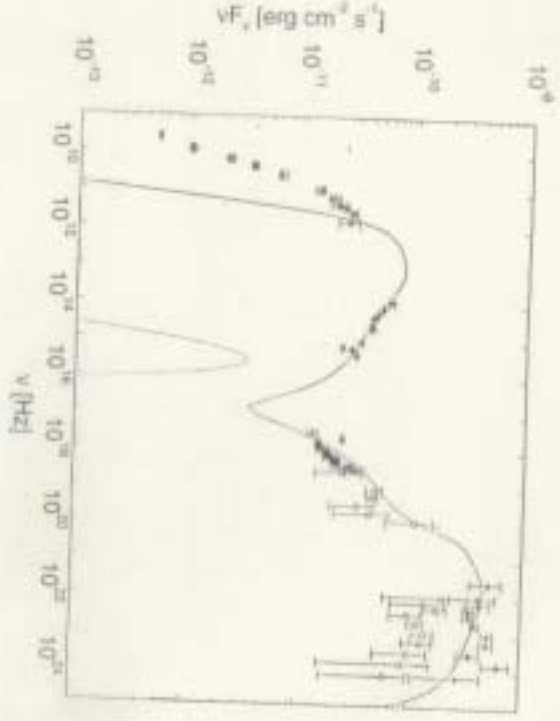

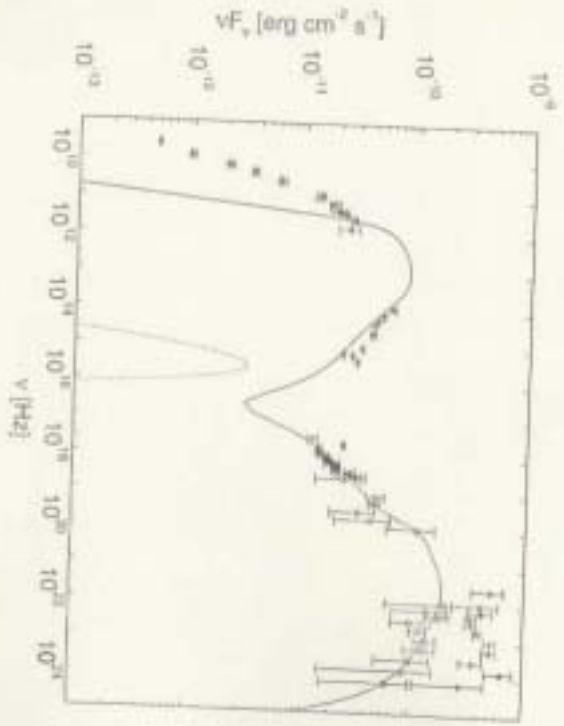

II. Standard model

- Adiabatic shock wave forms, properties of shock wave determined by MHD shock relations including sometimes nonlinear back reaction of accelerated particles

- Test particle acceleration by diffusive shock wave acceleration ⇒ power law distributions in rigidity of relativistic protons and pairs

- Total energy in accelerated particles from equipartition arguments $W_p = \alpha \frac{B^2}{8\pi}$

- Synchrotron-, SSC-, and external Compton cooling of pairs in optically thin case ($\tau_T n_e r \ll 1$) to explain multiwavelength spectra and light curves

- Optically thick case (proton-synchrotron cascade, pair cascade) more complicated

- Simple leptonic cooling models are successful to explain multiwavelength spectra of AGN jets and GRBs, but have difficulties with TeV light curves of Mrk 501 and Mrk 421

- Particle acceleration at relativistic shock waves even in the test particle limit not fully understood (universal spectral index 2.23 ± 0.01 differs from the spectral index needed for radiation modelling)

⇒ closer inspection of microphysics necessary

III) Theory of test-particle acceleration in relativistic and non-relativistic flows

Quasilinear ($\delta B \ll B_0$) approximation to cosmic ray particle's Boltzmann equation in mixed comoving frame (i.e. p, μ in fluid-frame; z, t in lab frame; $\vec{B}_0 = B_0 \vec{e}_z$):

1) Fokker-Planck equation for $f(p, \mu, z)$ in steady-state (Kirk, Schlickeiser, Schneider 1988; Webb 1989)

$$\Gamma(u + v\mu)\left[\frac{\partial f}{\partial z} - \frac{\partial u}{\partial z}\Gamma^2\left(m^2c^2 + p^2c^2\right)^{-1/2}\left(\mu\frac{\partial f}{\partial p} + \frac{1-\mu^2}{p}\frac{\partial f}{\partial \mu}\right)\right] \quad (1)$$

$$= S(f) + \mathcal{E}(f), \qquad \Gamma = \left(1 - \frac{u^2}{c^2}\right)^{-1/2}$$

$S(f)$: source term; $\mathcal{E}(f)$: wave-particle collision term

Scattering by parallel and antiparallel propagating Alfven waves:

$$\mathcal{E}_1(f) = \frac{\partial}{\partial \mu}\left[D_{\mu\mu}\frac{\partial f}{\partial \mu} + D_{\mu p}\frac{\partial f}{\partial p}\right] + \frac{1}{p^2}\frac{\partial}{\partial p}p^2\left(D_{\mu p}\frac{\partial f}{\partial \mu} + D_{pp}\frac{\partial f}{\partial p}\right)$$

$$D_{\mu\mu} = \sum_{\zeta=\pm 1} D(\zeta), \quad D_{\mu p} = \sum_{\zeta=\pm 1}\frac{\zeta\epsilon p}{(1-\zeta\mu\epsilon)}D(\zeta), \quad D_{pp} = \epsilon^2 p^2 \sum_{\zeta=\pm 1}\frac{D(\zeta)}{(1-\zeta\mu\epsilon)^2}$$

$$D(\zeta) = \frac{\pi}{2}\frac{R^2}{v B_0^2}\frac{(1-\zeta\mu\epsilon)^2}{|\mu-\zeta\epsilon|}\left[I_L^5\left(-\frac{1}{R_L(\mu-\zeta\epsilon)}\right) + I_R^5\left(\frac{1}{R_L(\mu-\zeta\epsilon)}\right)\right]$$

with $\epsilon = \frac{v_A}{v}$, $R_L = \frac{v}{|\Omega|}$

depends on power spectra $I^5_{4\pi}(k_\parallel)$ of fw, bw, RH and LH Alfven waves

2) Diffusion – Convection – Equation for isotropic phase space density $F(p,z)$ in steady-state:

for non-relativistic flows ($u \ll c$)

$$u\frac{\partial F}{\partial z} - \langle S\rangle = \frac{\partial}{\partial z}\left(K\frac{\partial F}{\partial z}\right) + \left(\frac{p}{3}\frac{\partial u}{\partial z} + \frac{\partial \beta_1}{\partial z}\right)\frac{\partial F}{\partial p}$$

$$- \frac{1}{p^2}\frac{\partial}{\partial p}\left(p^2\beta_1\right)\frac{\partial F}{\partial z} + \frac{1}{p^2}\frac{\partial}{\partial p}\left(p^2 a_2 \frac{\partial F}{\partial p}\right) \qquad (2)$$

with pitch-angle averages: $\langle g(\mu)\rangle \equiv \frac{1}{2}\int_{-1}^{+1} d\mu\, g(\mu)$

$$\kappa = \frac{v^2}{4}\left\langle \frac{(1-\mu^2)^2}{D_{\mu\mu}}\right\rangle \qquad \text{spatial diffusion}$$

$$\beta_1 = \frac{v}{2}\left\langle \frac{(1-\mu^2)D_{\mu p}}{D_{\mu\mu}}\right\rangle \qquad \text{rate of adiabatic deceleration}$$

$$a_2 = \left\langle D_{pp} - \frac{D_{\mu p}^2}{D_{\mu\mu}}\right\rangle \qquad \text{momentum diffusion}$$

Note: 1) For relativistic flows, equivalent to Eq. (2) more complicated mathematical structure than diffusion – convection type

2) cosmic ray convection speed

$$V = u + \frac{1}{p^2}\frac{\partial}{\partial p}\left(p^2\beta_1\right) \neq u$$

different from gas speed! Determined by relative intensities of forward and backward moving waves: $u - V_A \leq V \leq u + V_A$

3) Existing research on Fokker-Planck-equation:
(Kirk, Schneider 1987; Drury, Heavens, Achterberg, Gallant, Duffy, Gallmann and others ....):

for review see Kirk+Duffy 1999, J. Phys. G 25, R163

- neglect $D_{\mu p}$ and D_{pp} (higher order in $\epsilon = \frac{V_A}{v}$)
- step function profile $u = \begin{cases} u_+ & \text{in } z>0 \\ u_- & \text{in } z<0 \end{cases}$

  so that $\frac{\partial u}{\partial z} = 0 \quad \forall z \neq 0$
- solve

$$\Gamma_\pm^2\left(u_\pm + v\mu\right)\frac{\partial f_\pm}{\partial \mu} = \frac{\partial}{\partial \mu} D_{\mu\mu}\frac{\partial f_\pm}{\partial \mu}$$

at both sides of the shock by eigenfunctions (of $D_{\mu\mu}$) expansion and match solutions at $z=0$:

$$f_+(p,\mu,z=0) = f_-(p,\mu,z=0)$$

- adopt simple forms of $D_{\mu\mu}$:

(i) isotropic $D_{\mu\mu} = d_0(1-\mu^2)$ (Kirk+Schneider 87)

(ii) $D_{\mu\mu} = (1-\mu^2)\left(\mu^2 + 0.01\right)^{1/3} d_0(p)$ (Heavens+Drury 88)

being the same at both sides of the shock
$\left(d_0^+(p) = d_0^-(p) = d_0(p)\right)$

- use shock properties from relativistic MHD

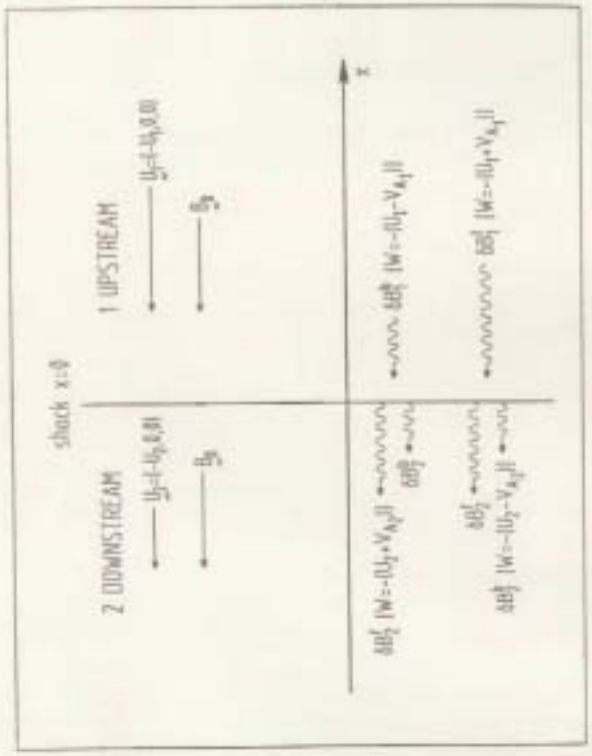

Fig. 16.1

IV) Test-particle acceleration at non-relativistic parallel shocks

(Vainio, Schlickeiser, Campeanu, Lerche)

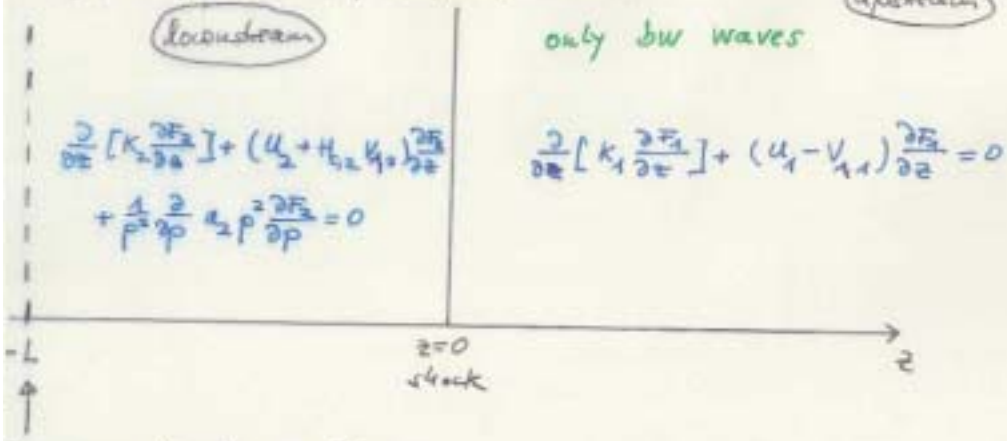

free-escape boundary condition

$F_2(z=-L)=0$

1) Specify upstream conditions : only bw-moving Alfven waves

⇒ cosmic ray bulk speed $V_1=-(U_1-V_{A1})$

no momentum diffusion $a_{2,1}=0$

2) Use Rankine-Hugoniot-relations to <u>calculate</u> downstream conditions from upstream conditions

⇒ shock generates both fw and bw Alfven waves downstream (relative intensities given by cross helicity H_{c2})

⇒ downstream cosmic ray bulk speed $V_2=-(U_2-V_{A2})$,

$a_{2,2}=a_2\neq 0$

3) At shock ($z=0$) : $F_1(0,p)=F_2(0,p)$

$$\left[K_1\frac{\partial F_1}{\partial z}+(U_1-V_{A1})F_1\right]_{0^+}-\left[K_2\frac{\partial F_2}{\partial z}+(U_2-V_{A2})F_2\right]_{0^-}$$

$$+\frac{U_1-V_{A1}-(U_2-V_{A2}H_{c2})}{3p^2}\frac{\partial}{\partial p}\left[p^3F_1(0,p)\right]+q_0(p)=0$$

1) Shock equations (Rankine-Hugoniot-relations)

continuity of normal magnetic field and tangential electric field, ($\vec{B} = \vec{B}_0 + \delta\vec{B}$ including Alfven waves):

$$[B_n]_1^2 = 0 \quad , \quad [\vec{B}_t u_n - B_n \vec{u}_t]_1^2 = 0$$

conservation of mass and perpendicular momentum:

$$[\rho u_n]_1^2 = 0, \quad [\rho \vec{u}_t u_n - \phi \frac{B_n \vec{B}_t}{4\pi}]_1^2 = 0$$

conservation of parallel momentum:

$$[\rho u_n^2 + P_{11} + (2\phi - 1)\frac{B_t^2}{8\pi}]_1^2 = 0$$

conservation of energy:

$$[\{\frac{\rho}{2}u_n^2 + \frac{5P_0}{2} + (\phi-1)\frac{B_n^2}{4\pi}\}u_n + \{\frac{\rho}{2}u_t^2 + (2\phi-1)\frac{B_t^2}{4\pi}\}u_n - \phi B_n \frac{\vec{u}_t \cdot \vec{B}_t}{4\pi}]_1^2 = 0$$

Alfven-wave property: $\delta\vec{u}^{\pm} = \mp \phi^{1/2} \frac{\delta\vec{B}^{\pm}}{(4\pi\rho)^{1/2}}$

Vainio+Schlickeiser 2001: anisotropic gas pressure

$$\phi = 1 - \frac{4\pi}{B^2}(P_0 - P_1) \quad \text{upstream}, \ \phi_2 = 1$$

Vainio+Schlickeiser 1999, 1998; Schlickeiser, Campeanu, Lerche 1992: $\phi = 1$

2. Results ($\phi = 1$): 1) $D_{\mu\mu}^{(1)} \neq D_{\mu\mu}^{(2)} \Rightarrow K_2 \neq K_1$

2) cosmic ray compression ratio

$$r_K = \frac{V_1}{V_2} = \frac{u_1 - V_{A1}}{u_2 + H_{c2} V_{A2}} \neq \frac{u_1}{u_2} = r$$

can be much larger than r!

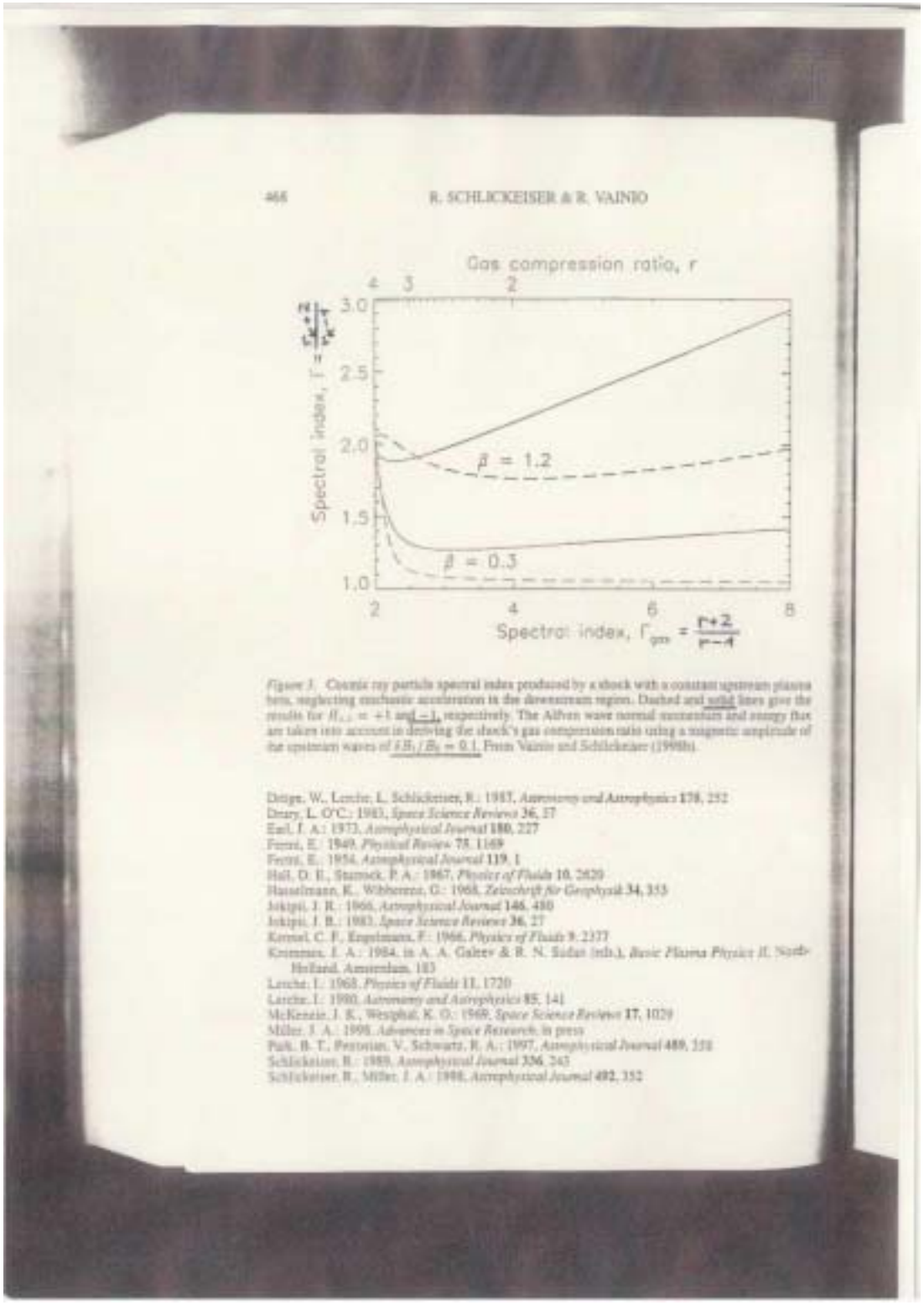

466 R. SCHLICKEISER & R. VAINIO

Figure 3. Cosmic ray particle spectral index produced by a shock with a constant upstream plasma beta, neglecting stochastic acceleration in the downstream region. Dashed and solid lines give the results for $H_{\pm\pm} = +1$ and -1, respectively. The Alfven wave normal anisotropy and energy flux are taken into account in deriving the shock's gas compression ratio using a magnetic amplitude of the upstream waves of $\delta B_1 / B_0 = 0.1$. From Vainio and Schlickeiser (1998b).

Dröge, W., Lerche, I., Schlickeiser, R.: 1987, *Astronomy and Astrophysics* **178**, 252
Drury, L. O'C.: 1983, *Space Science Reviews* **36**, 57
Earl, J. A.: 1973, *Astrophysical Journal* **180**, 227
Fermi, E.: 1949, *Physical Review* **75**, 1169
Fermi, E.: 1954, *Astrophysical Journal* **119**, 1
Hall, D. E., Sturrock, P. A.: 1967, *Physics of Fluids* **10**, 2620
Hasselmann, K., Wibberenz, G.: 1968, *Zeitschrift für Geophysik* **34**, 353
Jokipii, J. R.: 1966, *Astrophysical Journal* **146**, 480
Jokipii, J. R.: 1983, *Space Science Reviews* **36**, 27
Kennel, C. F., Engelmann, F.: 1966, *Physics of Fluids* **9**, 2377
Krommes, J. A.: 1984, in A. A. Galeev & R. N. Sudan (eds.), *Basic Plasma Physics II*, North-Holland, Amsterdam, 183
Lerche, I.: 1968, *Physics of Fluids* **11**, 1720
Lerche, I.: 1980, *Astronomy and Astrophysics* **85**, 141
McKenzie, J. K., Westphal, K. O.: 1969, *Space Science Reviews* **17**, 1029
Miller, J. A.: 1998, *Advances in Space Research*, in press
Park, B. T., Petrosian, V., Schwartz, R. A.: 1997, *Astrophysical Journal* **489**, 358
Schlickeiser, R.: 1989, *Astrophysical Journal* **336**, 243
Schlickeiser, R., Miller, J. A.: 1998, *Astrophysical Journal* **492**, 352

3) shock equation for compression ratio $r = \frac{s_2}{s_1}$ including Alfvén waves: $b = (\delta B_1 / B_0)^2$

$$(M^2 - r)^2 \{2r\beta - M^2[\gamma + 1 - (\gamma - 1)r]\}$$

$$+ b M^2 r \{(\gamma - 1)r^2 + [M^2(2-\gamma) - (\gamma+1)]r + \gamma M^2\} = 0$$

for adiabatic gas $P S^{-\gamma} = \text{const.}$, plasma beta $\beta = \frac{\Sigma P_1}{S_1 V_{A1}^2}$, Alfvénic Mach number $M = u_1 / V_{A1}$

consequences: (i) for $b = 0$

$\Rightarrow$ switch-on shock solution $r = M^2$

and $r = \frac{\gamma + 1}{\gamma - 1 + \frac{2\beta}{M^2}}$ standard shock solution

(ii) for $b \neq 0$: no switch-on solution exists!

4) Full solution including free-escape boundary L_2 and momentum diffusion for $I_1 \propto K_{11}$ given by Schlickeiser, Campeanu and Lerche (1992):

for large Peclet numbers $\frac{V_2 L}{K_2} \gg 1$

momentum spectrum of accelerated particles

$N(p) \propto p^{-\Gamma}$, $\Gamma = \frac{r_K + 2}{r_K - 1}$

determined by first-order Fermi process,

$\Gamma < 2$ (Limit $\Gamma \to 1$ for $r_K \to \infty$) because $r_K > 4$

for many parameters (excellent for flat synchrotron spectra $\alpha < 0.5$!)

D. Green (2001)

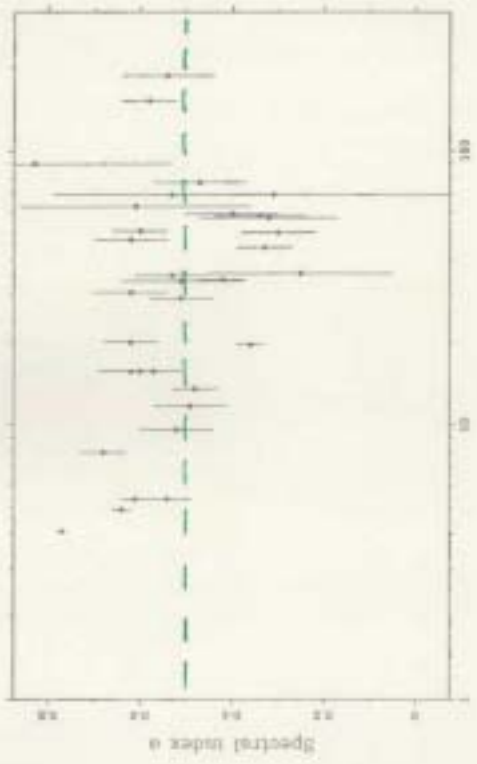

FIGURE 5. Plot of radio spectral index against diameter for Galactic shell SNRs.

This accounts for much of the correlation shown in the $\Sigma - D$ relation in Fig.4. Undoing this D^{-2} bias, and plotting the $L - D$ relation — also shown in Fig.4 — shows that there is wide range of luminosities shown by SNRs for all diameters.

RADIO SPECTRA OF SNRS

Here I use the convention that the radio spectral index, α, is defined so that the observed radio flux density varies with frequency ν as $\nu^{-\alpha}$ (which corresponds to a synchrotron emission from an underlying population of energetic particles scaling with energy as $\propto E^{-2\alpha+1}$). The radio spectra of SNRs can be summarised by the generalisation that "SNRs have a spectral index of 0.5, as expected from Fermi

V) Clues from non-relativistic shock acceleration work

1) Microphysics of plasma wave–shock interaction is important not only for resulting momentum spectrum of accelerated particles but also for shock wave structure.
(upstream power spectrum $I_1(k_{\parallel}) \propto k_{\parallel}^{-q}$, q ?
ratio of fw to bw waves, polarization state, non-parallel wave propagation)

Gas compression ratio is different from ~~shock~~ scattering center compression ratio !

2) Cosmic ray transport parameters
($D_{\mu\mu}, D_{\mu p}, D_{pp}$ for Fokker-Planck-equation;
κ, β_1, a_2 for diffusion-convection-equation)
have to be calculated, and they are different downstream from upstream!

⇒ Consequences for relativistic shock acceleration theories ?!

Is analytic work still possible, or are we left with simulations only ?

3) Dynamics of plasma waves is crucial (their generation and interaction with relativistic outflows).
⇒ Alternative simplified model : relativistic pick-up model

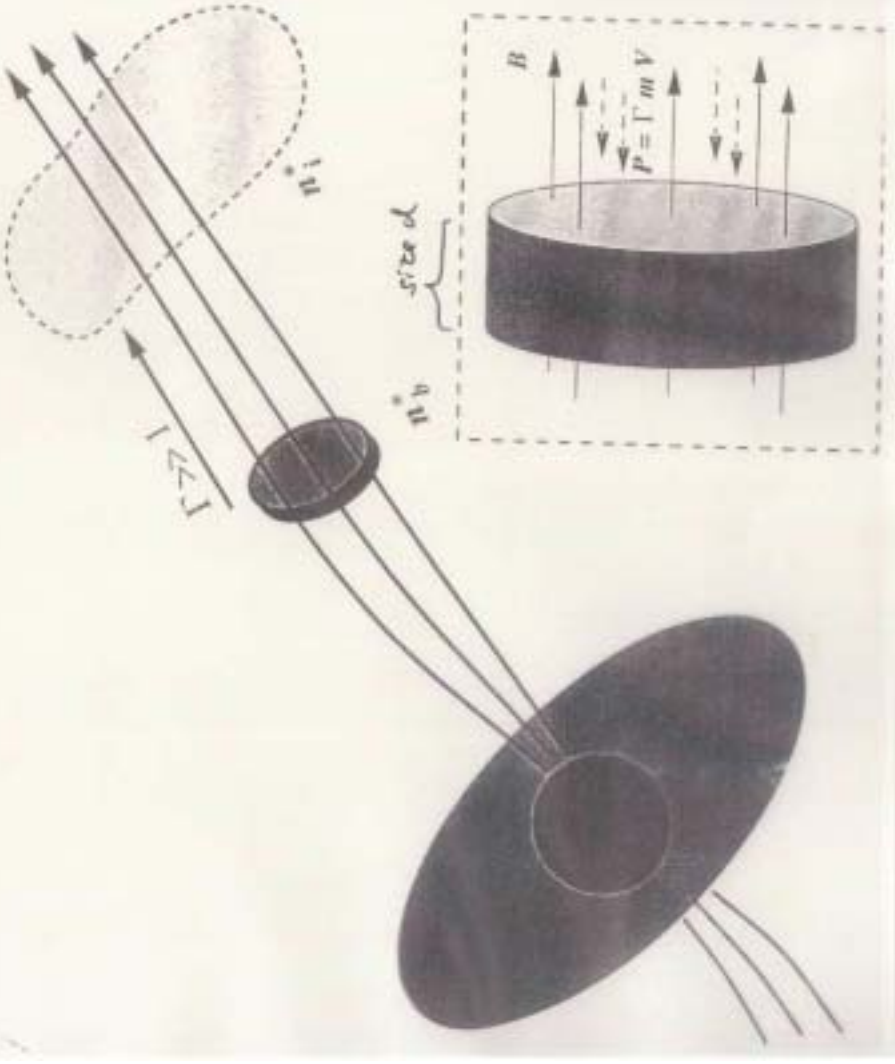

Relativistic pick-up model

II) Relativistic pick-up model

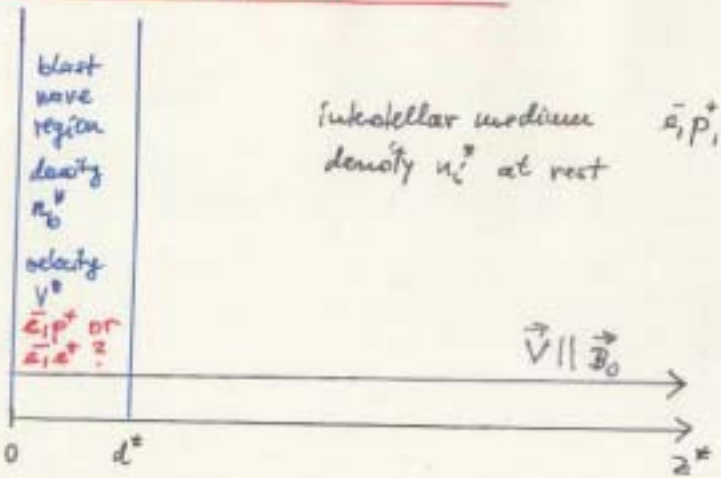

interstellar medium e^-, p^+ ($d\bar{d}$)
density n_i^* at rest

Plasma parameters :

Source type	blast wave composition	density $n_b^*(cm^{-3})$	interstellar medium density $n_i^*(cm^{-3})$
Supernova	p^+, e^-	10^3	1
GRBs	e^+, e^- p^+, e^-	$10^{17} - 10^{14}$	1
AGNs	p^+, e^- e^+, e^-	10^9	1

VI. Relativistic pick-up model

Initial state $t=0$

In lab-frame thermal blast-wave plasma, density n_b^*, propagates with speed $\vec{V} \parallel \vec{B}_0$ into cold e-p interstellar medium of density $n_i^* \ll n_b^*$.

Blast-wave plasma consists either of pairs (e^+, e^-) or $e^- - p$.

Viewed in blast-wave rest frame:

$$n_b = n_b^*/\Gamma' \quad , \quad n_i' = n_i^* \Gamma' \quad , \quad \Gamma' = \left(1 - \frac{v^2}{c^2}\right)^{-1/2}$$

For $\frac{n_i'}{n_b} = \frac{\Gamma'^2 n_i^*}{n_b^*} = 10^{-4} \frac{\Gamma_{100}^2 n_i^*}{n_{b,0}^*} \ll 1 \Rightarrow$ weak beam

of interstellar incoming p^+ and e^- :

$$f(\vec{p}, t=0) = n_i' f_i'(p, \mu, t=0) + n_b f_b(p, \mu, t=0)$$

$$= \frac{n_i'}{2\pi p^2} \delta(\mu - 1)\, \delta(p - P) + n_b \frac{\exp\left[-\frac{\sqrt{1 + \frac{p^2}{m_e^2 c^2}}}{\Theta}\right]}{4\pi (m_e c)^3 \Theta K_2\left(\frac{1}{\Theta}\right)}$$

where $P = mc(\Gamma^2 - 1)^{1/2}$, $\Theta = \frac{k_B T_{pair}}{m_e c^2}$

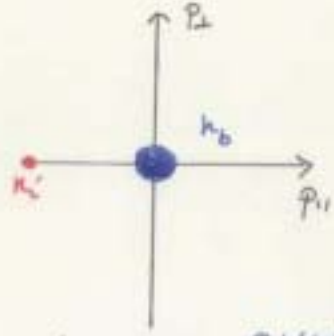

unstable (2-stream instability) initial state,

what happens at later times ?

(pair blast wave : Schlickeiser, Vainio, Böttcher, Lerche, Pohl, Schuster 2002
p-e blast wave (cold) : Pohl, Schlickeiser 2000
Pohl, Lerche, Schlickeiser 2001)

Beam excites

longitudinal electrostatic waves ($\delta E \gg \delta B$) :

$$\frac{\partial I_e(K,t)}{\partial t} = 2\psi_e I_e(K,t), \quad \psi_e \propto \int d^3p \frac{\partial f_i'}{\partial p_\parallel} \delta($$

$$\frac{\partial f_i'(p_\parallel, p_\perp, t)}{\partial t} = \pi e^2 \frac{\partial}{\partial p_\parallel} \left[\int_{-\infty}^{\infty} dK\, I_e(K,t)\, \delta\left(\omega_R - \frac{K p_\parallel}{g m_i'}\right.\right.$$

that "plateau" ($\frac{\partial f_e}{\partial p_\parallel} = 0$) the incoming fa p^+ and e^- and heat the blast wave plasma on time scale t_e.

transverse Alfven waves ($\delta B \gg \delta E$) : $\omega_R^2 = 1$

(+) fw and (-) bw mooring

$$\frac{\partial I_\pm(K,t)}{\partial t} = \pm 2\psi I_\pm(K,t), \quad \psi \propto \int d^3p \frac{\partial f_i'}{\partial \mu} \delta($$

$$\mu_0 \simeq -$$

$$\frac{\partial f_i'}{\partial t} = \frac{\partial}{\partial \mu} D_{\mu\mu} \frac{\partial f_i'}{\partial \mu}, \quad D_{\mu\mu} \propto \int_{-\infty}^{\infty} dK\, I_\pm(K,t)\, \delta(\pm V_e$$

that isotropize the incoming p^+ and e^- on time

Efficient pick-up or capture of interstellar particles

growth rates ψ_e and $|\psi|$ much larger than t Landau and cyclotron damping rates for E

Electrostatic instability quicker than transv instability : $t_e \ll t_s$

Sequence of evolution

Initial state (t=0) :

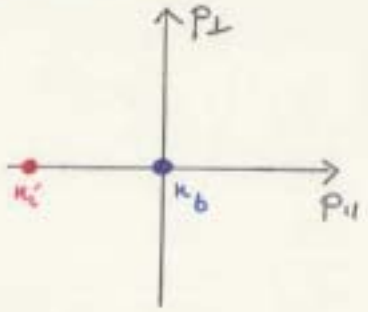

Plateau state ($t = t_e$) $\frac{\partial f}{\partial p_\parallel} = 0$ of incoming p^+, e^-

$\frac{(\delta E)^2}{8\pi} = \frac{1}{2} \Gamma n_i' m_p c^2 (1 + \frac{m_e}{m_p})$

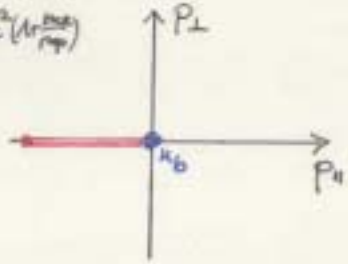

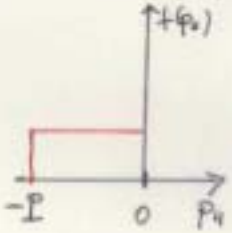

$I = \Gamma n_i' V$

Isotropic sphere state ($t = t_e + t_s$) $\frac{\partial f}{\partial p} = 0$ for $p \simeq P$

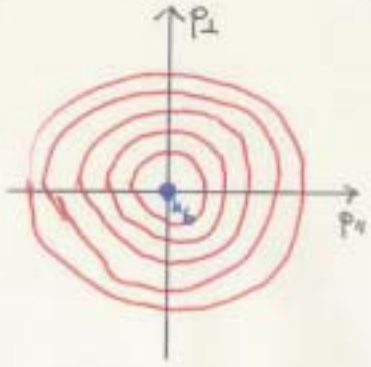

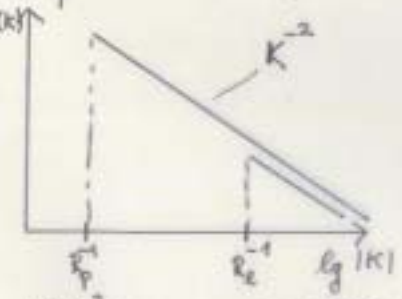

$2 \frac{(\delta B)^2}{8\pi} \frac{1}{2} n_i' m_p V_A V \Gamma (1 + \frac{m_e}{m_p})$

$= \frac{1}{2} \frac{V_A}{c} n_i' m_p c^2 \Gamma (1 + \frac{m_e}{m_p})$

If isotropisation time scales

$$t_{s,p} = 430 \frac{(n_{b,p}^*)^{1/2}}{n_i^* \Gamma_{100}^{1/6}} \; s, \quad t_{s,e} = 0.02 \frac{(n_{b,p}^*)^{1/2}}{n_i^* \Gamma_{100}^{1/6}}$$

are shorter than the light crossing time of the blob

$$t_l = \frac{d}{c} = 3 \cdot 10^4 \, l_{13}^* \, \Gamma_{100} \; s$$

⇒ blast wave picks up interstellar p^+ and e^- with

$E_{max,p} = \Gamma m_p c^2 = 100 \text{ GeV } \Gamma_{100}$ (primary energy output at TeV energies ⇒ $E_{max,p}^* = 10 \text{ TeV } \Gamma_{100}^2$)

$E_{max,e} = \Gamma m_e c^2 = 0.5 \text{ GeV } \Gamma_{100}$

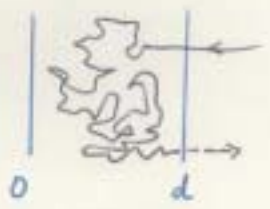

In blast-wave region isotropized (interstellar) p^+ and e^- interact with thermal blast wave particles (e^+-e^- or p^+-e^-).

Random walk of isotropized p^+, e^- ⇒ spatial diffusion

⇒ escape time

$$t_{esc} = \frac{d^2}{K} = \frac{3d^2}{c^2 t_s} = 3 \frac{t_e^2}{t_s}$$

$$t_{esc,p} = 7 \cdot 10^6 \frac{(l_{13}^*)^2 \, \Gamma_{100}^{13/6} \, n_i^*}{(n_{b,p}^*)^{1/2}} \; s, \quad t_{esc,e} = 1.5 \cdot 10^{11} \frac{(l_{13}^*)^2 \, \Gamma_{100}^{13/6} \, n_i^*}{(n_{b,e}^*)^{1/2}} \; s$$

p^+-e^- blast wave is thick target for interstellar p

if $t_{pp} = \frac{1.7 \cdot 10^9}{n_{b,p}^*} \Gamma_{100} \; s < t_{esc,p}$

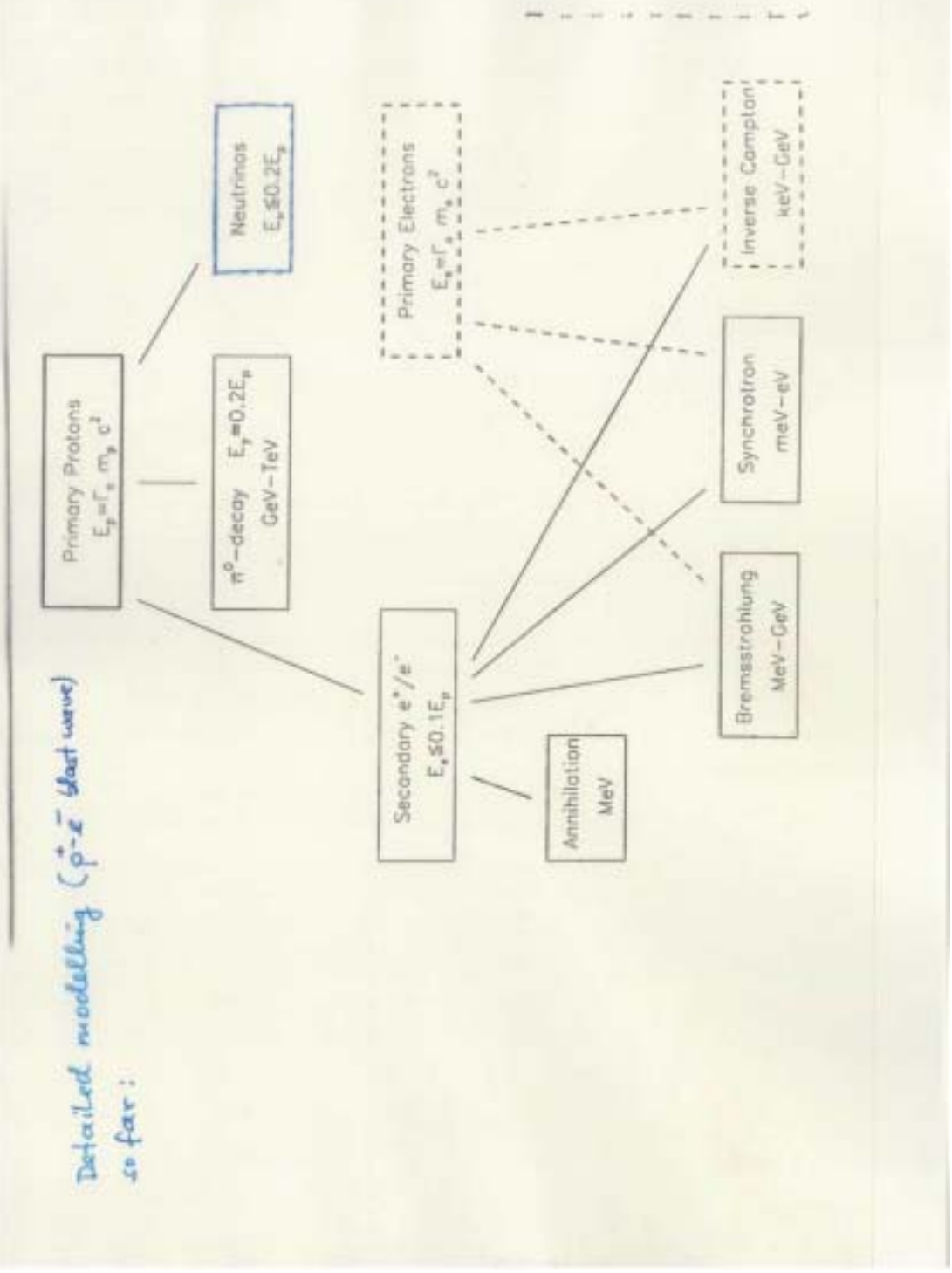

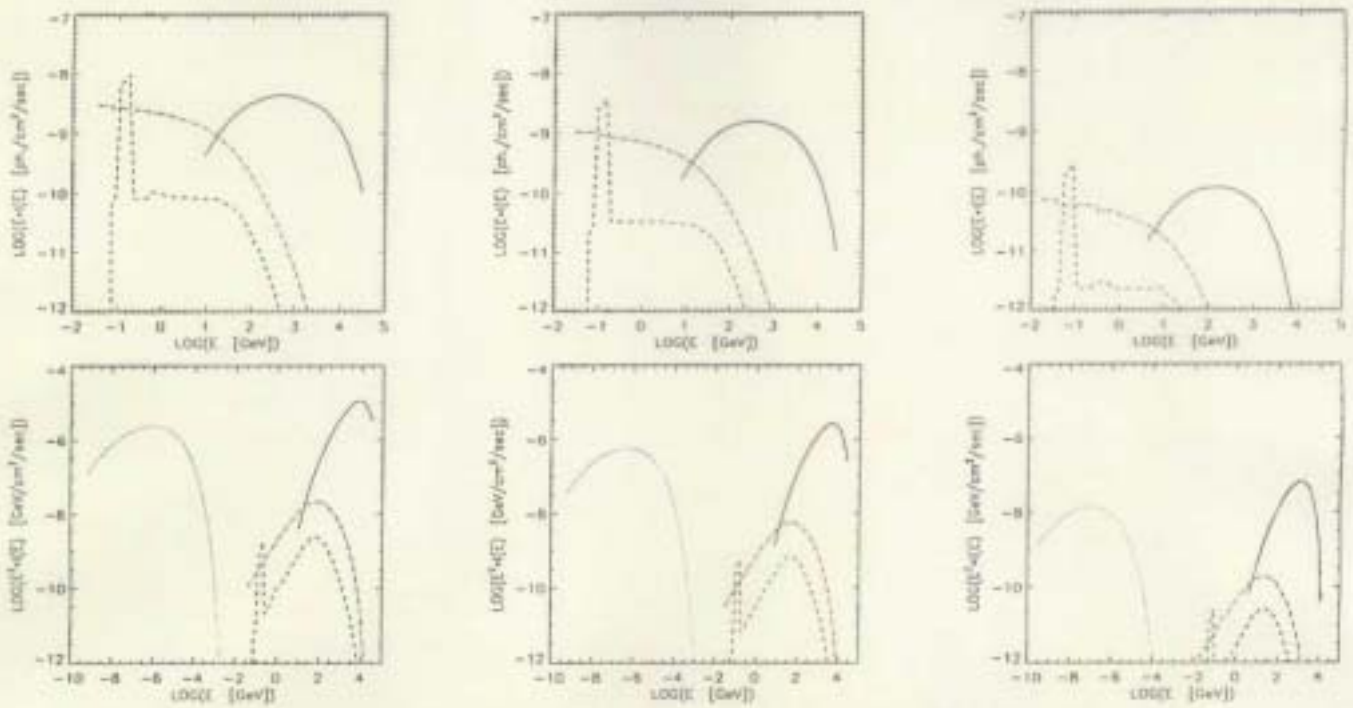

Fig. 4. Spectral evolution of a relativistic blast wave in an environment of constant density. The top row displays F_ν spectra of the γ-ray emission, whereas the bottom row shows νF_ν spectra from the optical to high energy γ-rays including also the synchrotron emission. The solid lines display π^0-decay γ-rays, the dot-dashed lines bremsstrahlung, the dashed lines annihilation emission, and the dotted lines represent the synchrotron emission. From left to right the panels show the spectra after one hour, 10 hours, and 100 hours observed time. The parameters are: Γ_0=300, d=3 · 10^{13}cm, R=10^{14}cm, B= 2.0 G, n_e^*=0.2 cm^{-3}, n_{th}=5 · 10^8 cm^{-3}, for an AGN at z=0.5 viewed at an angle $\theta_{obs} = 0.1°$. After 100 hours the blast wave has decelerated to $\Gamma \simeq 106$.

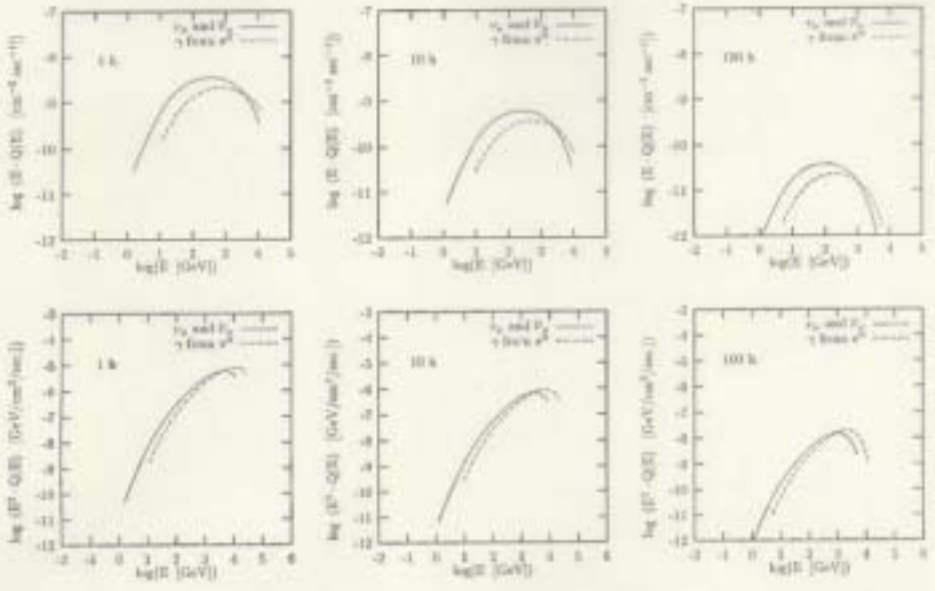

Fig. 6. The evolution of the muon neutrino emission resulting from the proton spectra of Fig. 2. The viewing angle is $\theta = 0.1°$ and the redshift of the AGN is $z = 0.5$. All the other parameters are chosen as in Fig. 2. In the top row we see the F_ν spectra and in the bottom row the νF_ν spectra. The spectral evolution of the γ-ray production spectra is also shown for reference.

collision process as well as the relativistic ones. The approximation for the source function $Q_\nu(\gamma_p, t)$ is:

$$Q_\nu = \int_1^\infty \frac{N(\gamma_p, t)}{\tau} \left(\delta(\gamma_p - \frac{\gamma}{2}) + \delta(\gamma_p - 1.1) \right) d\gamma_p \qquad (24)$$

with $\tau = 3 \cdot 10^{16}\ n_e^{-1}$. The second δ-function with the assumed 1.1 accounts for the thermal protons. Again we

4. The evolution of the neutrino emission spectra in comparison with γ-ray production

In this paper we focus on the high energy muon neutrino emission resulting from the decay mode of pions $\pi^+ \to \mu^+ + \nu_\mu(\bar{\nu}_\mu)$ and subsequently $\mu^+ \to e^+ + \bar{\nu}_\mu + \nu_e(\bar{\nu}_e)$.

In Fig. 6 and Fig. 7 we show two examples of spectral evolution of total muon neutrino emission calculated with the model proton spectra seen in Fig. 3 and in Fig. 5. We

Böttcher, R.S., Marra 2001

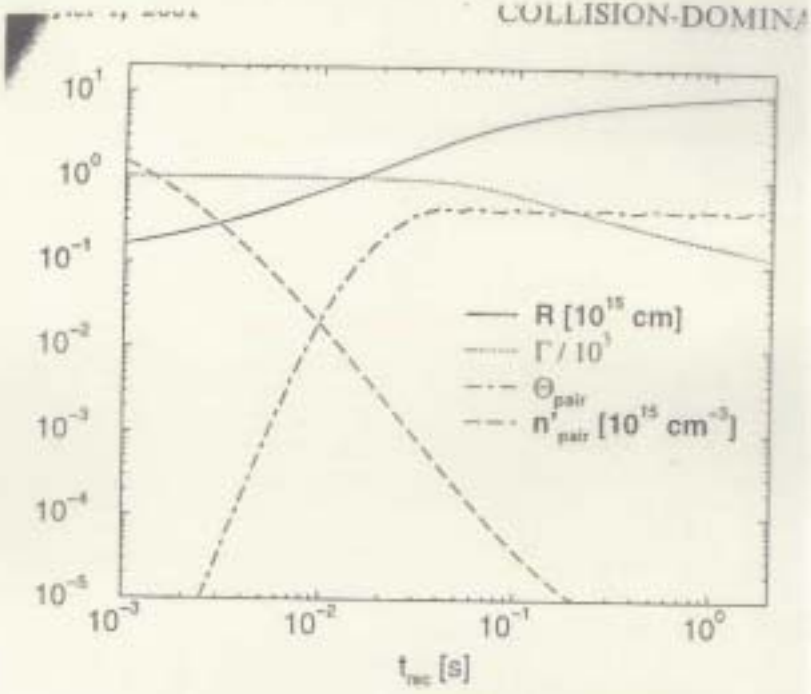

FIG. 6.—Time evolution of several relevant quantities describing the evolution of the plasmoid, for the same set of parameters as in Fig. 4.

BSM 2001

Böttcher, Schlickeiser, Marra 2001

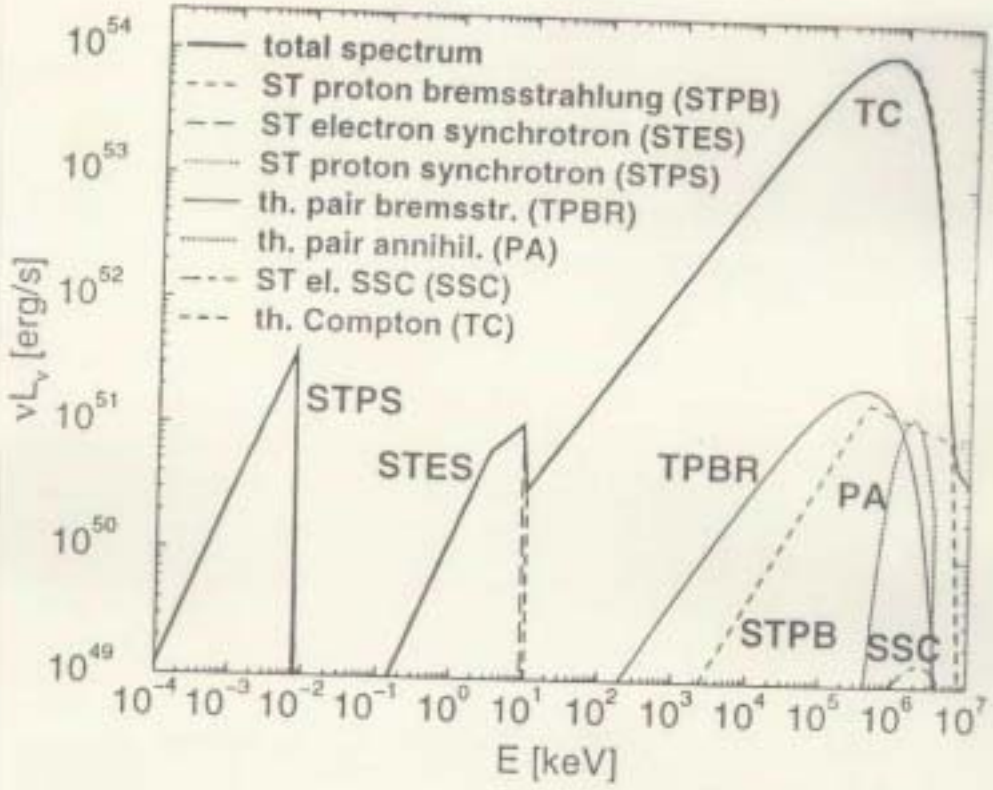

FIG. 4.—Composite photon spectrum from the blast wave at the time of maximum received flux ($t_{rec} = 64$ ms). Parameters for this simulation are $\Gamma_0 = 10^3$, $n'_{pair} = 1.2 \times 10^{16}$ cm^{-3}, $R_0 = 10^{14}$ cm, implying $\tau_{T,0} = 1$, $n_{ISM} = 100$ cm^{-3}, $\epsilon_B = 0.1$, $\theta_{obs} = 0$. $\gamma\gamma$ absorption has been taken into account to calculate the total emission, while the individual contributions are plotted without correction for $\gamma\gamma$ absorption. Thus, the importance of $\gamma\gamma$ absorption and pair production is illustrated by the difference between

BSM 2001

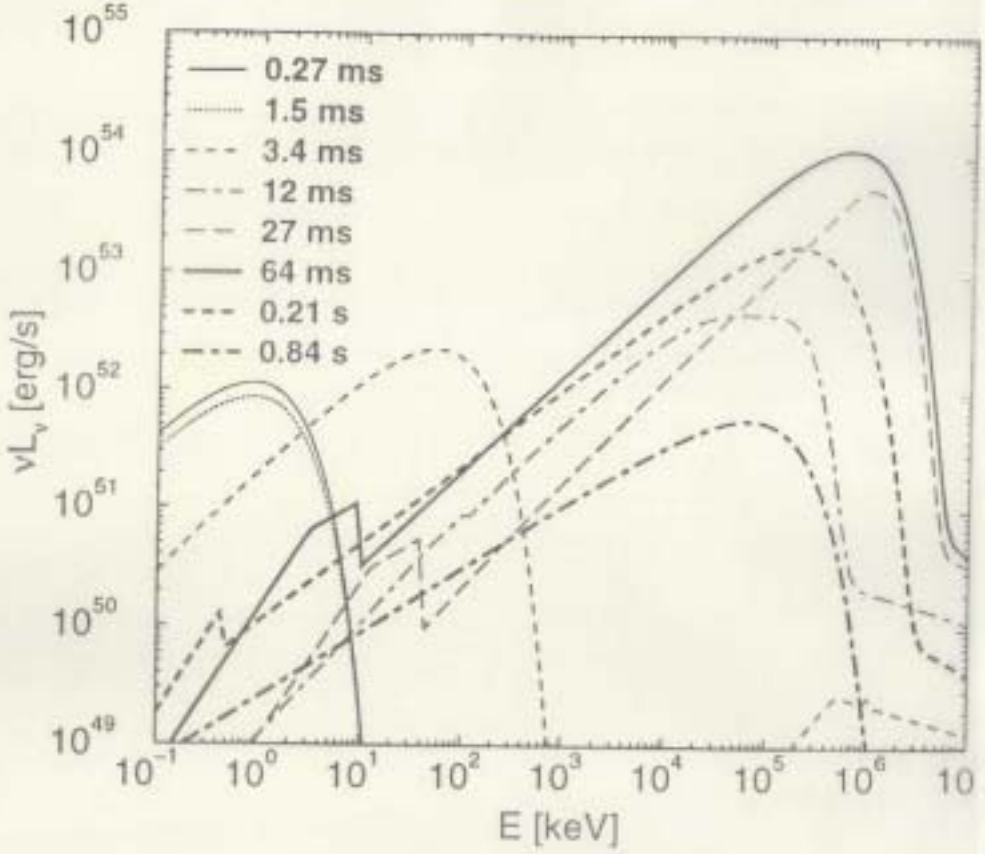

FIG. 5.—Time evolution of the observed photon spectra for the sam set of parameters as in Fig. 4.

BMS 2001

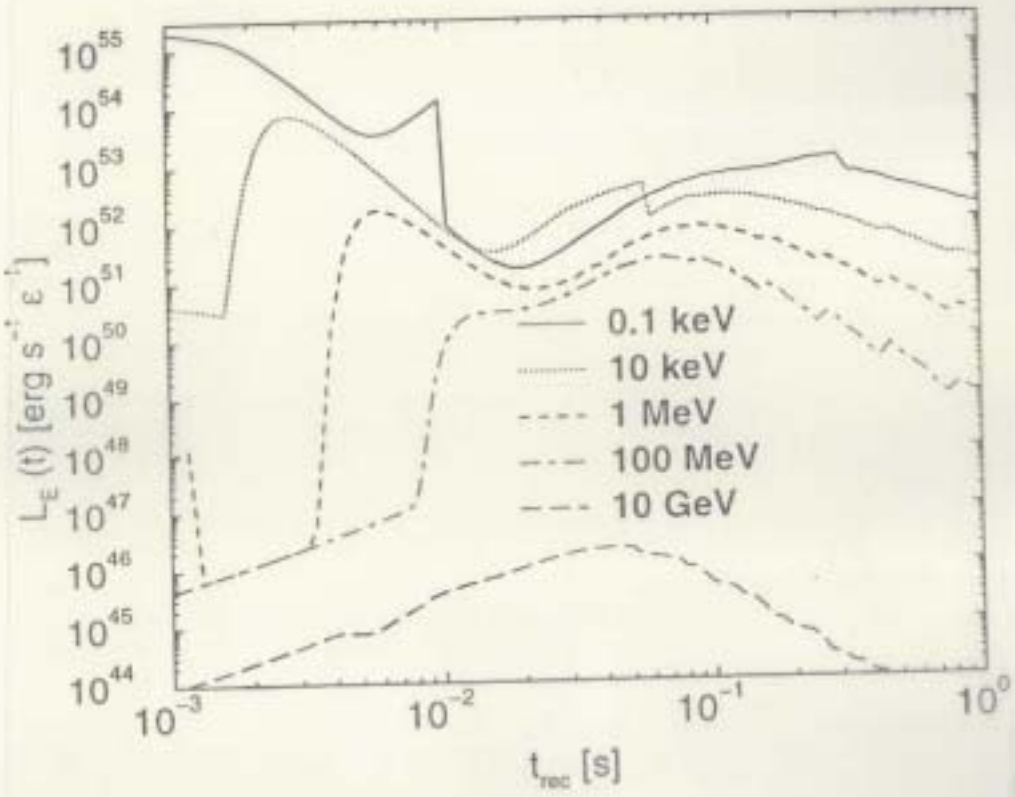

FIG. 7.—Light curves at several different observed photon energies fo the same set of parameters as in Fig. 4.

$p^+ e^-$ - blast wave :

- p^+ carry 1836 more energy than primary e^-
- protons produce pions ($\pi^0, \pi^\pm$) with $\Gamma_\pi \approx \Gamma_p$ $\Rightarrow E_p = 30\ \Gamma_{100}^2$
- $\pi^0 \to 2\gamma$ with $E_{\gamma max} = m_\pi c^2 \cdot 30\ \Gamma_{100}^2$, in forward direction observer in "lab-system" sees photons with $E_{\gamma max} = 2\Gamma\ E_{\gamma max}^* = 0{,}9\ \Gamma_{100}\ TeV$
  i.e. primary energy release in "TeV photons !)
- $\pi^\pm$ - decays produce secondary neutrinos and secondary $e^+ e^-$

⇒ Doppler-boosted neutrino emission at TeV energies in phase with TeV photons (Jokipii, Rodi, Schlickeiser 07)

⇒ Synchrotron radiation of secondary $e^+ e^-$ at optical - X-ray energies multiwavelength spectra of AGN jets

- If blast wave runs through inhomogeneous interstellar medium $n_i^*(\vec{x}) \neq$ const ⇒ expansion of TeV light curve

Pair ($e^+ e^-$) blast wave !

- p^+ still carry 1836 more energy than primary e^- but no π^0-gamma rays, no secondary $e^\pm$, no neutrinos due to lack of inelastic p-p collisions
- radiation channels much simpler !
  P radiate only by supra-thermal bremsstrahlung and synchrotron radiation
  primary e^- radiate by inverse Compton scattering, bremsstrahlung, annihilation, synchrotron radiation
- but efficient heating of blast wave pair plasma by Coulomb interactions and adiabatic waves

Radiation Channels (pair blast wave)

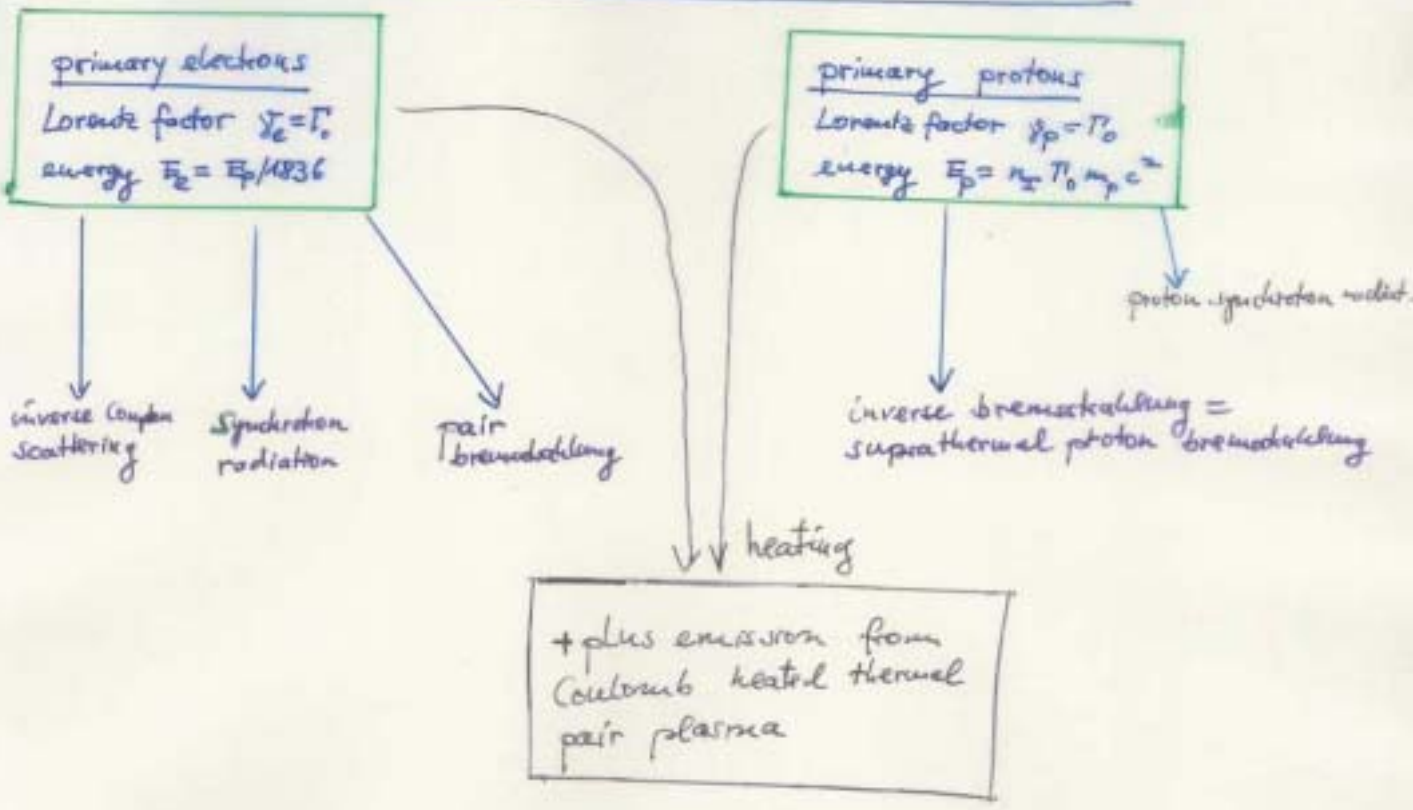

VII. Impact of future TeV observations

How can GeV–TeV-observations of AGN jets and their modelling guide acceleration theories?

Because observations do not resolve the shock wave region spatially, calculate time evolution of volume averaged momentum spectrum of captured interstellar particles

$$N_i'(p,t) = \int_0^d dz \int dx \int dy \; 4\pi p^2 f_i'(z,x,y,t,p) :$$

$$\frac{\partial N_i'}{\partial t} + \frac{\partial}{\partial p}(\dot{p}\, N_i') + \frac{N_i'}{T} = q_i'(p,t)$$

continuous losses: $\dot{p}(p,t)$ — escape: $T(p,t)$ — injection

Position of emission blob: $z = z_0 + Vt$

Acceleration theories predict different injection rates:

shock acceleration $q_i' = c_1 N_i'^*(t)\, p^{-s}$, $p > p_c$

relativistic pick-up $q_i' = c_2 N_i'^*(t)\, p^2$, $p < P = mc\sqrt{p^2+1}$

With solution $N_i'(p,t)$ for equilibrium spectrum determine photon fluxes and/or fluences at different frequencies and light curves

$$N_i'(p,t) = \frac{1}{|\dot{p}|} \int_{-\infty}^{t} dt_0 \int_0^{\infty} dp_0 \, q_i'(p_0,t_0) \exp\left[-\int_{t_0}^{t} \frac{dt'}{T(p,t')}\right] \delta\left(\int_{p_0}^{p} \frac{dp'}{\dot{p}(p',t')} - t + t_0\right)$$

VIII. Conclusions

1) Work on nonrelativistic shock acceleration demonstrates that microphysics of plasma wave–shock interaction is crucial both for shock wave structure in a collision-pure magnetized medium and for momentum spectrum of accelerated particles.

It is not the gas compression ratio that determines the power law spectral index of accelerated particles, but the scattering center compression ratio, and these are different.

2) Cosmic ray transport parameters, in particular $D_{\mu\mu}$, are different upstream and downstream of the shock. This should have consequences also for relativistic shocks.

3) Test-particle transport equations have been formulated, but we need more analytic solutions for correct transport parameters e.g. $D_{\mu\mu}^{(1)} \neq D_{\mu\mu}^{(2)}$.

4) Simplified models of plasma wave generation and interaction (e.g. relativistic pick-up) in relativistic outflow sources predict primary energy release at GeV–TeV photon energies.

5) Radiation modelling of AGN jets might give clues on relevant injection process (shock or pick-up).